Design and fabrication of a coherent array of single-mode optical fibers for the nulling coronagraph

Duncan T. Liu*, B. Martin Levine, Mike Shao
Jet Propulsion Laboratory, California Institute of Technology, 4800 Oak Grove Drives, Pasadena, CA, USA 91109

ABSTRACT

We present the development of a single-mode spatial filter array for the nulling coronagraph application. The development consists of two generations of fiber array designs and a Zygo-interferometer based lens array to fiber array alignment methodology. We discuss the use of large mode field diameter (MFD) fibers to relax fiber placement tolerance of the fiber array. The pros and cons of using the Photonic Crystal Fiber (PCF) for building the array are discussed. The future plan for implementing a 1000-channel class, single-mode spatial filter array is described.

Keywords: Coherent fiber array, micro-lens array, step-index single-mode fiber, photonic crystal fiber, spatial filter, Zygo interferometer, nulling interferometer, coronagraph

1. INTRODUCTION

Recently, a nulling interferometer coronagraph architecture was proposed to detect extra-solar planets at 10 pc away in the visible spectrum[1]. It consists of a single-telescope shearing interferometer, deformable mirrors for amplitude and phase control, and a single-mode spatial filter array. The pupil beam in the telescope is segmented into 4 beams, which are sheared and overlapped in such a way that the beams that are parallel to the optical axis (starlight) interfere destructively, while the beams that are not parallel to the optical axis (companion planet light) do not. To reduce the starlight to the required level so that the planet light is not washed out nearly perfect optical elements are required because imperfect optical elements cause wavefront mismatch between combined beams. A single-mode fiber spatial filter can circumvent this problem by transmitting only a single (lowest-order) fiber-guided mode; that is, after combined beams pass through the spatial filter, wavefront mismatch is automatically removed. The tradeoff of using a spatial filter is that it can affect the intensity balance between combined beams due to any differential fiber coupling efficiency.

A single-mode filter removes any spatial information in the incident beam. To preserve the spatial information of the incident beam while still perform single-mode spatial filtering, an array of single-mode spatial filter is required. To separate an earth-like planet from the parent star that is 10 pc away, a 4-meter telescope and a 1000-spatial filter array with a relative rms phase error less than 1/10 of a wave are needed. In this paper, we report the development of such a spatial filter array using single-mode fibers and micro-lens arrays as depicted in Figure 1. This includes two generations of fiber arrays. The first is a low-cost, best-effort, commercial fiber array used to develop the methodology of aligning and bonding lens arrays to the fiber array. The second is designed and fabricated in-house to improve the fiber placement accuracy. Using conventional visible single-mode fibers, the required fiber placement tolerance is very tight due to the relatively small Mode Field Diameter (MFD) of the fiber. We report the use of a large MFD Photonic Crystal Fiber (PCF) to circumvent this problem. Finally, we describe the future plan for implementing a 1000-channel class spatial filter array.

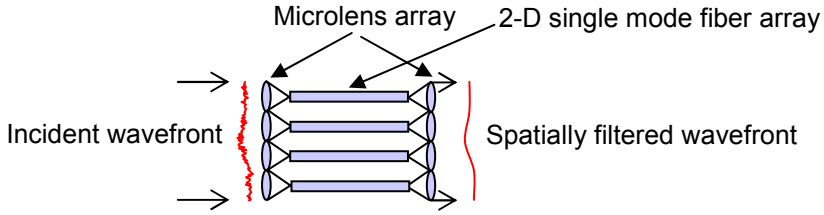

Figure 1: Single-mode spatial filter array using single-mode fiber and lens arrays.

*duncan.liu@jpl.nasa.gov; phone 1 818 354-9508; fax 1 818 393-4357; www.jpl.nasa.gov

2. STATE OF THE ART

2.1 Fiber arrays

The telecom industry has developed many fiber array products. However, they cannot be used for building spatial filter array directly. Most of them are 1-D fiber arrays developed for connecting to Dense Wavelength Division Multiplexing (DWDM) devices. A few of them are 2-D fiber arrays developed for connecting to 2-D Micro Electro Mechanical (MEMS) optical switch arrays. Placing fibers in 1-D V-groove arrays is the most popular method to implement 1-D fiber arrays. One way to implement a 2-D array is to stack these 1-D arrays. Another way is to etch an array of precision holes on a silicon wafer and insert the fibers into these holes to form a 2-D array. In both cases, the fiber core placement tolerance is between 1 to 2 µm for a 10 x 10 array. The v-groove based 2-D fiber array can be readily modified to have both sides polished, while the silicon wafer based fiber array requires more design change. The fiber core placement tolerance is not only determined by the hole and v-groove positions but also the concentricity of the core and cladding and the uniformity of fibers' cladding diameter, which are typically 0.5 to 1 µm. These tolerances are acceptable for telecom 1.3 µm or 1.5 µm single-mode fibers with a ~ 10 µm MFD, but they are not tight enough for existing visible wavelength single-mode fibers with a ~ 3 – 5 µm MFD. These tolerances become even tighter for building the 1000-channel class spatial filter array. A new approach described later in this paper may overcome this problem.

2.2 Lens arrays

Commercial lens arrays can be readily used for fabricating spatial filter array. The two lens array technologies used in this study are: (1) epoxy lens array deposited on glass substrate by Adaptive Optics Associates (AOA) and (2) gray scale etched fused silica lens array by MEMS Optical. Lens arrays can have a tighter placement tolerance (as small as 0.25 µm for MEMS Optical) than fiber arrays, in general. This makes it possible to fabricate a lens array with individual lens positions matching those of a specific fiber array.

3. PROPOSED APPROACH

3.1 Alignment methodology

The processes of aligning a lens array to a fiber array can be divided into two parts: (1) align the lens array and the end face of the fiber array to be parallel to each other and (2) align the lenslets to the fibers so that each focused beam is coupled into a fiber. We conceived a Zygo (or equivalent) interferometer based alignment methodology as illustrated in Figure 2 to perform these processes. A Zygo interferometer can measure the parallelism between a reflective surface and a reference flat to less than a fraction of a wave across the entire beam. The Zygo interferometer's beam diameter (~100 mm) we used is too large to measure the wavefront covering the area of one lens (~0.1 mm to 1 mm) even we use the built-in 6x zoom in the Zygo interferometer. This problem is partially circumvented by using a 20x beam expander. The 1:1 relay optics is to image the lens and fiber arrays on the beam expander's image plane located inside the beam expander. In addition, to align the lens array and the fiber array to be parallel within a few arc seconds we use a computer controlled 6-axis stage.

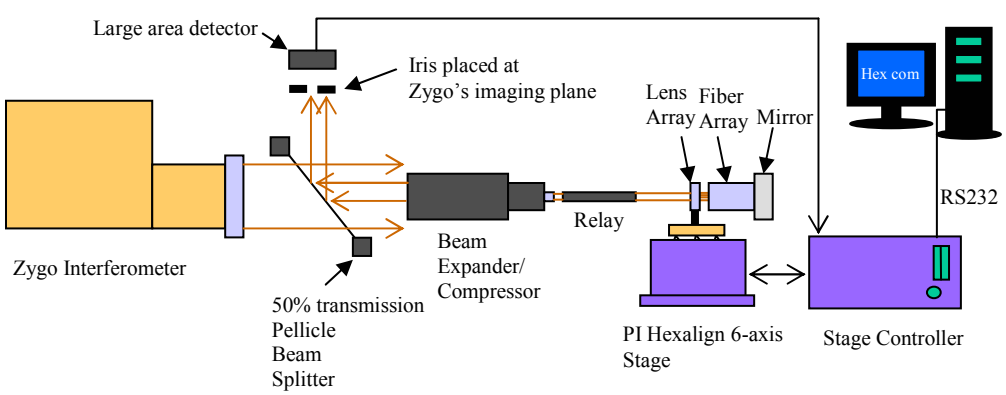

Figure 2: Schematic of lens array to fiber array alignment setup

To ensure the beam is perpendicular to the lens array and fiber array, we need to first align the reference flat of the Zygo interferometer to be perpendicular to the optical beam of Zygo interferometer using a corner cube (not shown);.note that the reflected beam from the corner cube is always parallel to the Zygo interferometer beam. Consequently, any surface aligned parallel to the reference flat is automatically perpendicular to the Zygo interferometer beam. In order to do so, the lens array and the fiber array need to have some reflectivity. We were able to carry out this process for an anti-reflection coated surface, which has a reflectivity of 0.25%.

In fiber coupling alignment processes, a mirror is first attached to the other end of the fiber array for reflecting coupled light back to the Zygo interferometer. The coupling alignment algorithm is illustrated in Figure 3. When a lenslet and a fiber are aligned, a bright spot appears on the monitor connected to the Zygo's internal CCD camera; It can also be detected by partially reflecting the wavefront with a pellicle beam splitter. To align the entire 2-D array, the lens array is first moved randomly until one lenslet is aligned to a fiber. The position of the lens on the 6-axis stage is recorded. Then the lens array is moved around until a second lenslet is aligned with a second fiber. This position of the lens array is also recorded. From these two positions and the separation of these two fibers, the angular misalignment between the lens array and the fiber array can be calculated. The 6-axis stage is then controlled to compensate the calculated angular misalignment. To speed up this process, one can also create some alignment marks on the fiber array and the lens array.

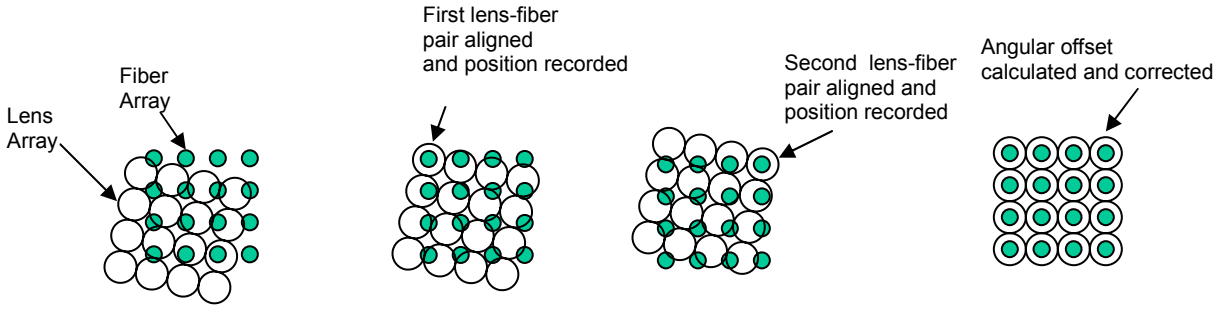

Figure 3: Illustration of lens array to fiber array alignment algorithm

3.2 Single-mode fibers considered

Three fibers are under consideration: (1) regular step-index, single-mode fiber (MFD ~ 3 to 4 μm), (2) large MFD single-mode PCF (MFD ~ 12 μm), and (3) large MFD, step-index, single-mode fibers (MFD ~ 12 μm). The first two fibers are off-the-shelf, while the third one requires custom-made fiber preform. So far, we have only performed experiments using the first two fibers and plan to investigate the third fiber in the next phase of development.

Figure 4 compares the fiber coupling lateral alignment sensitivity for a 4-μm MFD fiber with a 12-μm MFD fiber. The result shows the 12-μm MFD fiber is approximately 3 times less sensitive than a 4 μm MFD fiber. As the fiber array size becomes larger, the fiber's center-to-center placement needs to be more accurate so that the entire array can be aligned uniformly. For an array size of 1000 elements, a large MFD fiber is needed. While the use of large MFD fiber can relax the lateral alignment sensitivity, it increases the angular alignment sensitivity at the same time. However, the angular sensitivity of a Zygo interferometer that we use in aligning a lens array with a fiber array is much higher.

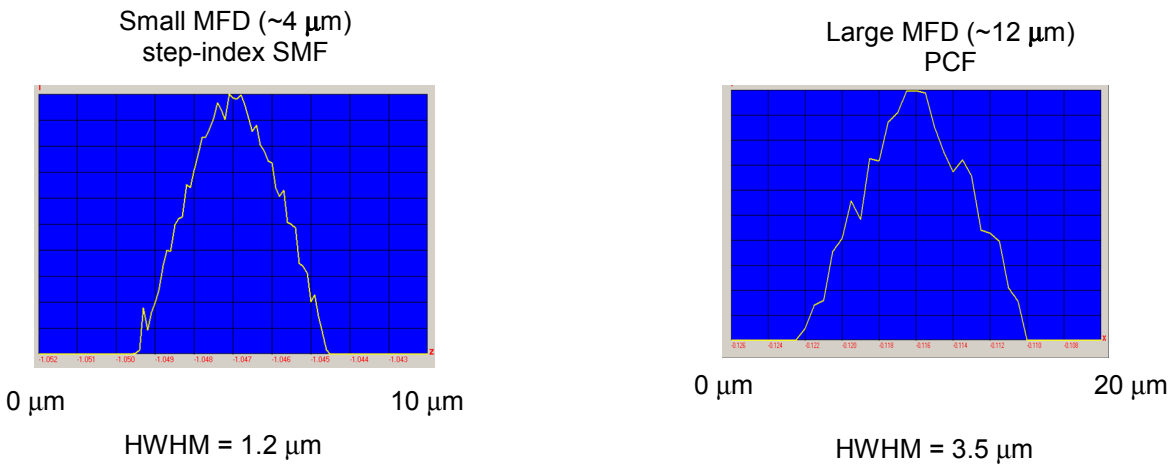

Figure 4: Alignment sensitivity comparison of small and large MFD fibers.

Large MFD PCF is the only commercial, large MFD, single-mode fiber available today. While the cladding and the core of a regular single mode fiber are made of glass with different refractive indices, PCF is made of glass with only one refractive index. The cladding of a PCF consists of many tiny air holes as shown in Figure 5. The mix of air and glass in the cladding creates an effective refractive index that is lower than that of the glass core. To polish a PCF, the two ends of the fiber need to be first sealed and cleaved. This service is fairly expensive due to the tight tolerance (50 μm) of the length between the two sealed ends. The process is further complicated by the need to align one end of fibers flush and the need to polish the fiber ends without exceeding the sealed sections on two ends. All these extra services are doable but expensive. Another unique feature of PCF is its MFD is nearly independent of wavelength over a large wavelength range. The coupling efficiency of a focused beam into a fiber is maximized when the focused airy diameter matches the MFD of the fiber. This feature implies that the fiber coupling efficiency of a PCF is not a flat curve of wavelength, while that of a conventional step-index single-mode fiber can be close to a flat curve over an Octave.

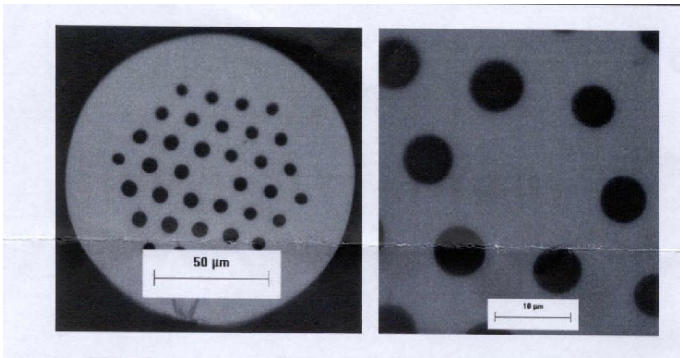

Figure 5: Cross section of PCF used in this research; courtesy Crystal Fibre A/S

Step-index single-mode fiber can be designed to have a larger MFD by using a smaller difference between the refractive indices of core and cladding. The cost of processing such type of fiber is much lower than PCF. However, it is not readily available commercially. We plan to acquire such a fiber in the next phase of fiber array development.

4. EXPERIMENTS

4.1 First generation fiber array using regular step-index fibers

The purpose of the first generation fiber array is to develop the alignment methodology. It is a custom commercial fiber array made of stainless-steel housing as shown in Figure 6. Due to the tolerance of machined parts, many gaps exist between fibers. The wavelength used in all experiments reported in this paper is 632.8 nm.

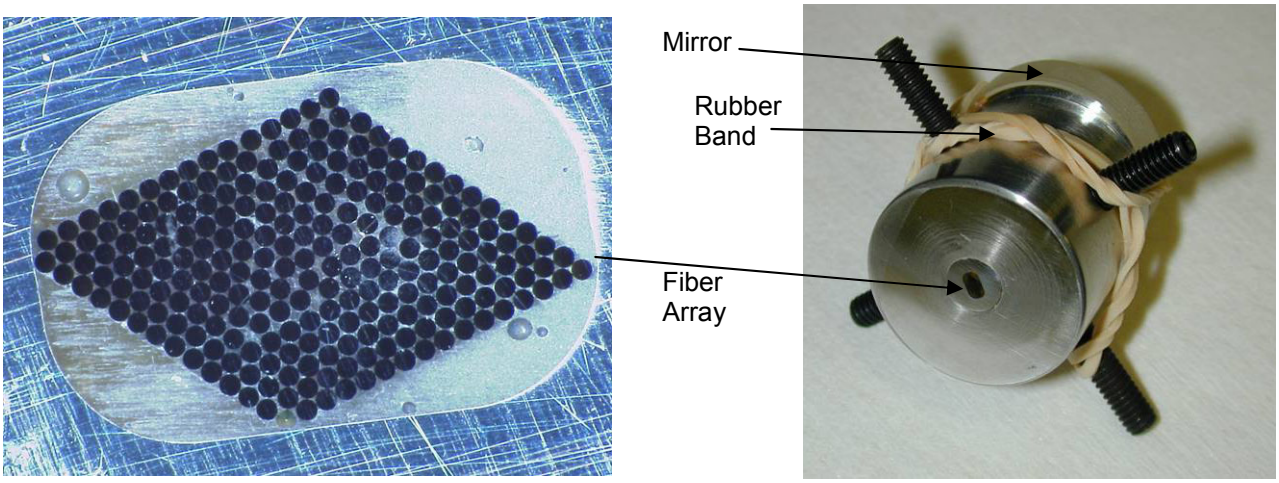

Figure 6: First generation fiber array. Mirror reflects coupled beams back for active alignment.

The fiber we used is a low birefringence single-mode fiber with an MFD of 3.5 µm at 633 nm and a cutoff wavelength at 600 nm. An off-the-shelf, F/4 lens array made by AOA as shown in Figure 7 was used to couple light into this fiber array. The pattern of the lens array is hexagonal, the lens spacing 125 µm, focal length 0.50 mm, substrate BK7 with 10 arc sec paralleled surfaces, substrate thickness 0.25", and the diameter of the substrate 1". To bond the lens array to the fiber array with one focal length away, a custom donut shaped BK7 spacer with the thickness equal to the focal length is bonded to the lens array on the side of substrate that has lenslets. The lens array is made of UV cured epoxy by molding. Anti-reflection coating (ARC) is deposited on the side of substrate without lens array only.

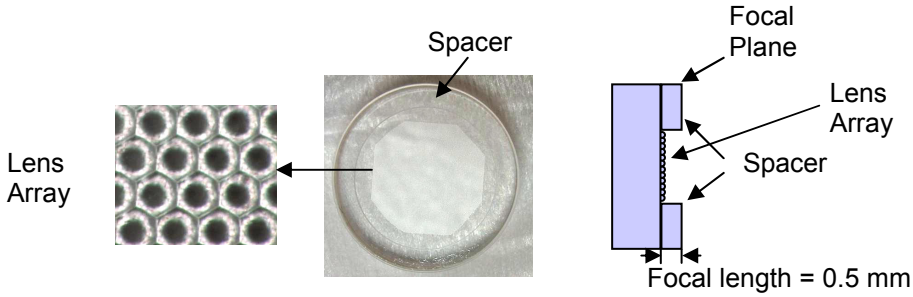

Figure7: AOA lens array with spacer. Drawing not to the scale

The lens array was characterized using the experimental setup described in 3.1 shown in Figure 8. As the lens array is characterized, a mirror was placed behind the lens array to reflect the focused beam back for measurement by Zygo interferometer. Although the reflected optical rays are not tracing the incident rays due to reflection, this checks the quality of the lens array to a good approximation. The actual quality of the lens array should be better than the results obtained with this method.

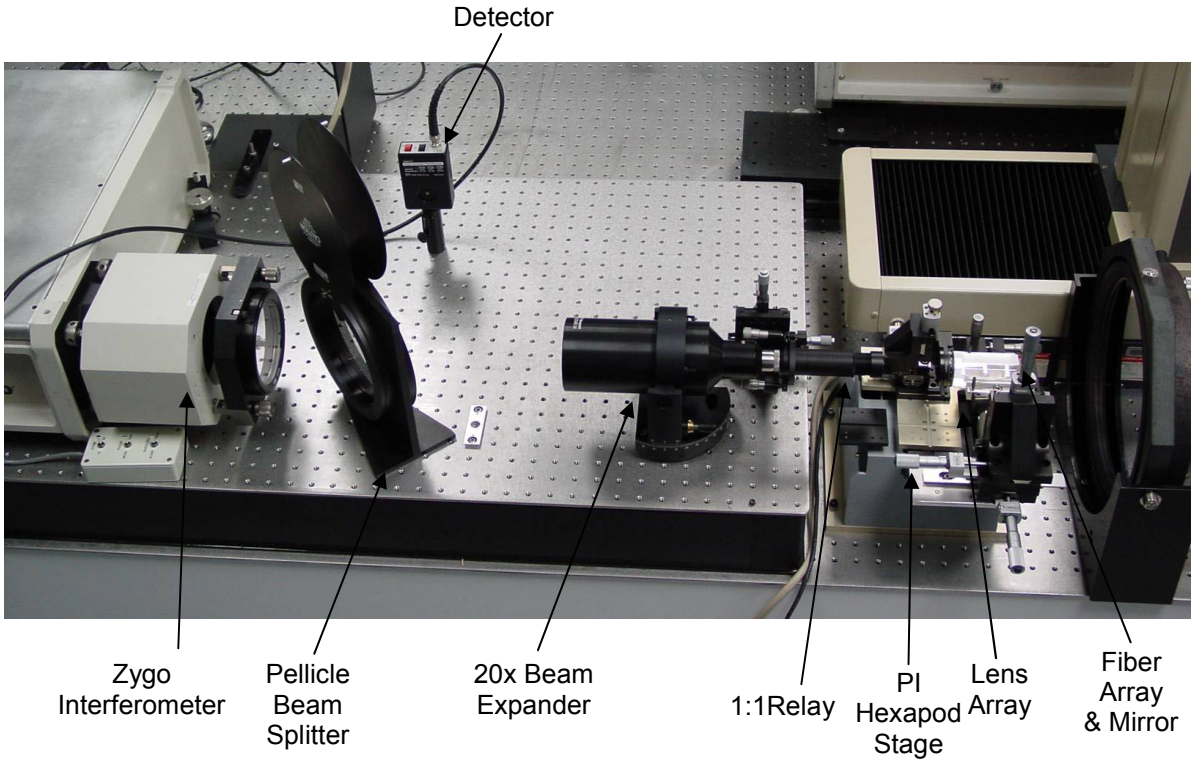

Figure 8: Experimental setup for aligning spatial filter array. Fiber array shown is the second generation.

To align the lens array to the fiber array, we attached a 1" mirror to the opposite end of the fiber array using a rubber band as shown in Figure 6. The mirror reflects any light that is coupled into the fiber and exits at the other end of the fiber back. The reflected beam exits the fiber and is recollimated by the lens array. This configuration is used on all lens array to fiber array alignment. The phases of the recollimated beams can then be measured against the reference flat of the Zygo interferometer. Figure 9 shows the rms relative phase of 7 beams to be 0.064 wave. This value corresponds to the wavefront passing through the lens array and fiber array once as it is corrected for double pass. This is one lens less than passing through the entire spatial filter. The rms relative phase for including the second lens array, to the first-order approximation would be approximately 1/3 more than the wavefront error obtained this way, assuming lens array and fiber array cause approximately equal wavefront errors.

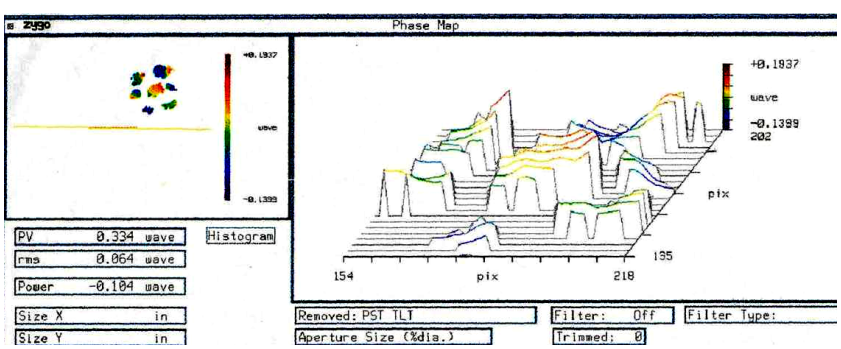

Figure 9: Phase map of 7 beams coupled out of the fiber array. PV= 0.334 wave, rms = 0.064 wave.

Figure 10a shows the near-field image of the fiber array without lens array; the other side has one lens array coupling light into the fiber array. Figure 10b shows the output mode of the fiber appears to be Gaussian; the core intensity to the cladding intensity was measured to be greater than 1000 : 1; the CCD camera we used has a dynamic range of 10,000 : 1.

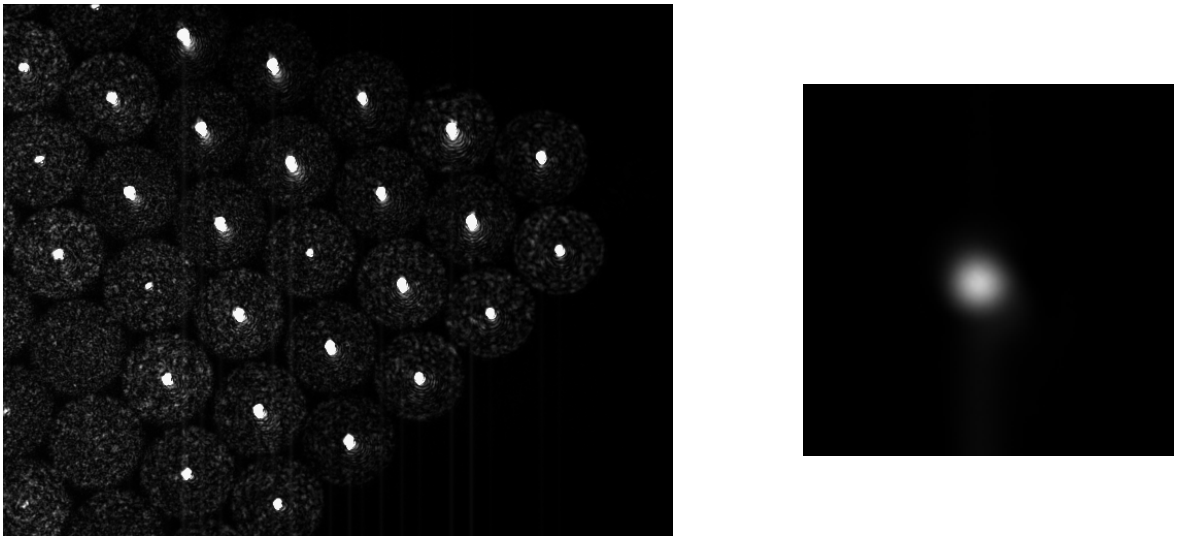

(a) (b)

Figure 10: (a) output beam pattern after some light coupled into fiber array, (b) Output fiber mode

4.2 Second-generation fiber array using regular step-index single-mode fiber

We designed a prism confined fiber array as shown in Figure 11. The key to this design is the equilateral triangle formed with the edges of three precision equilateral prisms. The inverted prism in the middle has a flat top. We implemented this design with two different fibers: step-index fiber and PCF.

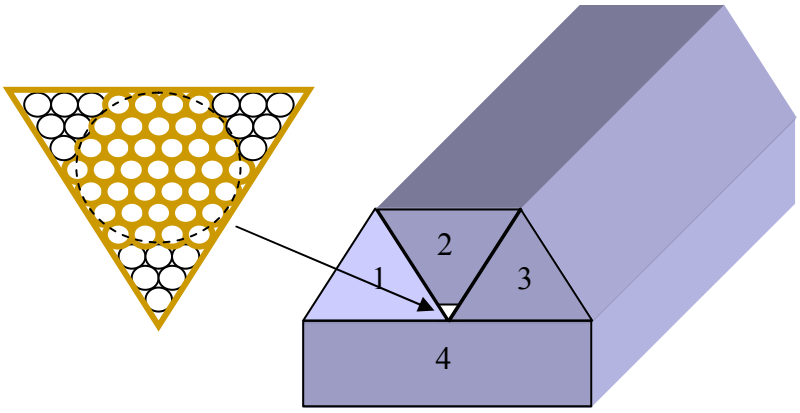

Figure 11: 3-D drawing of the second-generation fiber array design.

The purpose of making the conventional step-index single-mode fiber array is to develop the assembly process, since PCF is very expensive to prepare. The step-index fiber array uses the same fibers as in the first-generation fiber array. The assembled array is shown in Figure 12. The fibers and prisms are bonded with a low-viscosity, low-hardness, UV-cured epoxy. After assembly, the two ends of the fiber array are polished optically to have a reflected rms wavefront error < 1/10 wave and parallel to each other within 20 arc seconds.

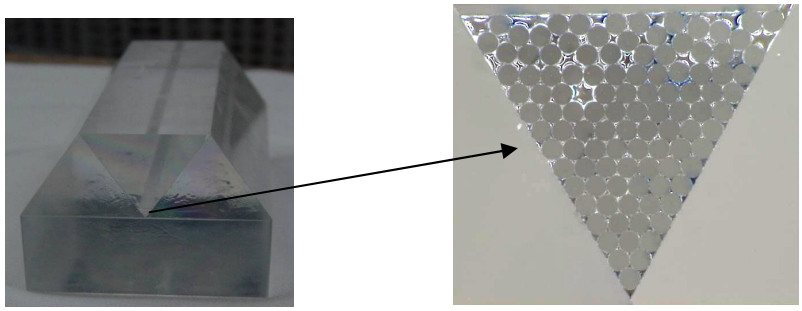

Figure 12: First second-generation fiber array with regular step-index single mode fibers

The fibers in the first 10 rows also from the bottom are aligned well. The top few rows are not aligned well. We believe we missed approximately one row on the top. This problem can be probably prevented if we have a layer of flexible material such as sponge placed between the flat top of the middle prism and the fiber array.

The lens array used to couple light into this fiber array is the same as the one used in the first generation fiber array described in 4.1. At the time of preparing this manuscript, we have not bonded the lens arrays to the fiber array. However, we have aligned one lens array to the fiber array with a mirror making contact with the other end of the fiber array. The reflected, double passed beam array is shown in Figure 13. More fibers have light coupled in than the first-generation lens-fiber array. This could mean the fibers in the second-generation fiber array are arranged more orderly than the first-generation one.

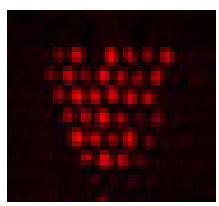

Figure 13: Far field image of output beams from the first second-generation fiber array.

Figure 14 shows the phase map of approximately 15 reflected double-passed beam array. The rms wavefront error of this array is 0.068 wave, which is about the same as that for 7 reflected beam array of the first-generation fiber array but with more fibers. Again, one needs to add approximately 1/3 to this wavefront error to take into account of the second lens array.

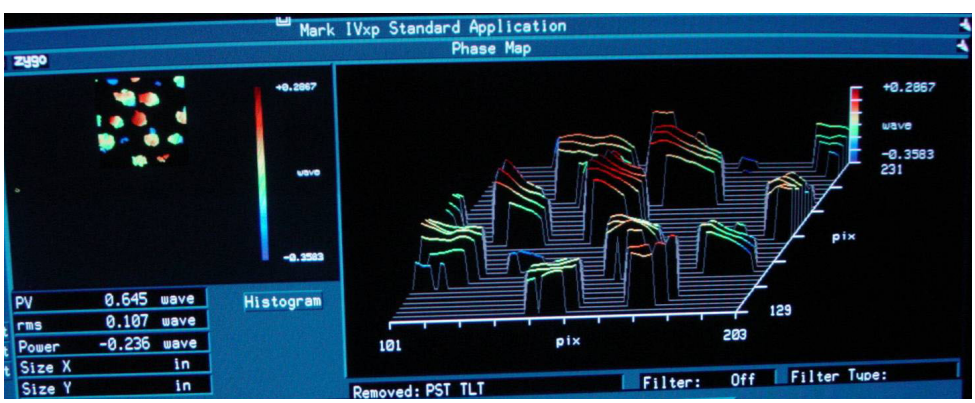

Figure 14: Phase map of approximately 15 coupled beams with a mirror on one side of the fiber array.

4.3 Second-generation fiber array using large MFD PCF

Due to the high cost of PCF, we only built an equilateral triangular array with 28 fibers. To polish the end face of a PCF, the air holes at the fiber ends need to be collapsed so that opaque debris will not plug them during polishing. The fibers also need to be cleaved into the same length within 50 to 100 nm so that the focus error distribution is within the depth of focus. The MFD of the fiber is approximately 12 μm. Figure 15 shows the two ends of the polished fiber array. Guided white illumination light can be seen in the core region. Surrounding air holes are visible in the cladding region shown in the left photo. Polishing may have caused the fiber edges irregular on this side of fiber array. This is improved when the other side was polished. The most possible reason for the forming of the visible gaps between fibers on both ends is that the middle flat-top prism was not pushed down enough during epoxy curing.

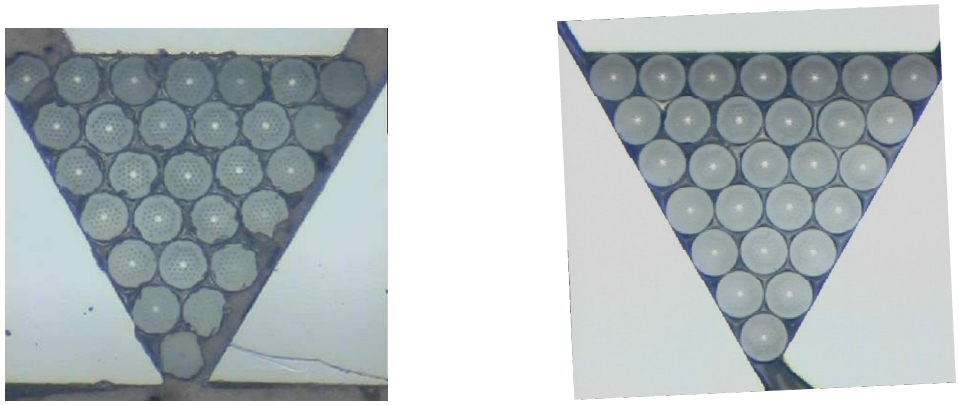

Figure 15: Two ends of the second-generation fiber array using PCFs.

Figure 16 shows the layout of a custom gray-scale etched lens array fabricated by MEMS Optical to match the MFD of the PCF array at the 632.8nm wavelength. Note that the lenslets of this lens array are located on the left side of the substrate and the incident beam is focused on the right side of the substrate, while the lenslets of the AOA's lens array are located on the right side of the substrate and the incident beam is focused in air (see Figure 7). With this new design the lens array can be bonded to the fiber array using an index-matching epoxy as illustrated in Figure 17. As a result, the irregular surface of the fiber array is not visible to incident wavefront any more. Figure 18 shows the phase map of the lens array measured with a mirror directly behind the lens array.

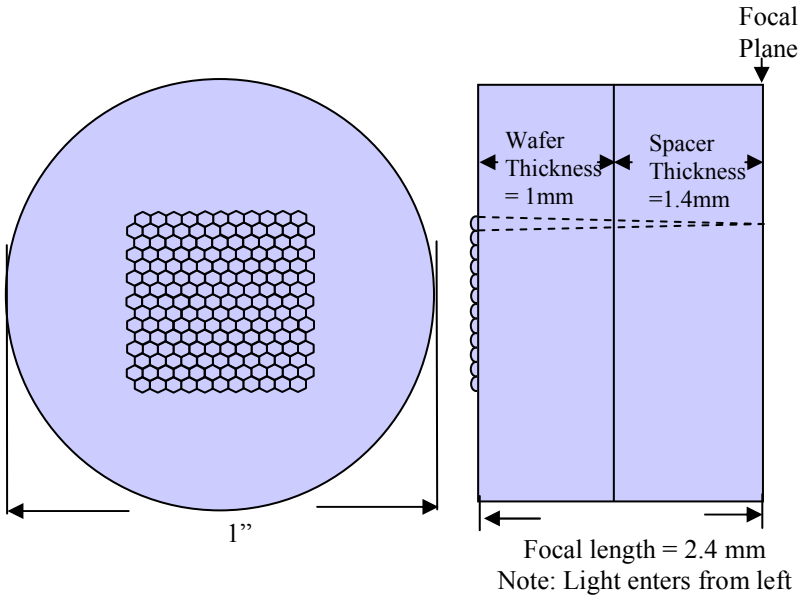

Figure 16: Lens array layout for PCF array. Drawing not to the scale.

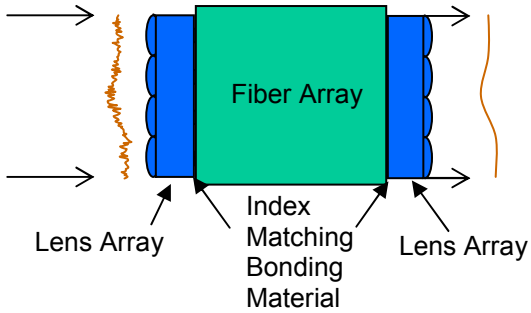

Figure 17: New lens array is designed to be bonded with fiber array without air gap.

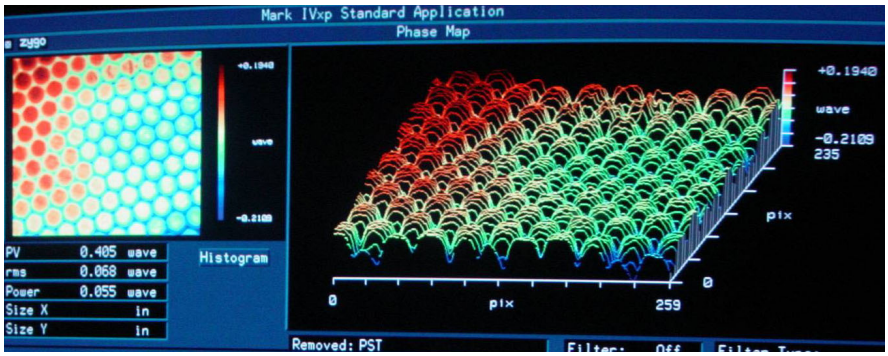

Figure 18: Phase map of custom MEMS Optical lens array.

The lens arrays have not been bonded to the PCF array yet at the time of submitting this paper. However, we have explored the characteristics of aligning one lens array to the fiber array with a flat mirror behind the fiber array. Figure 15 shows the existence of micron-level gaps between most fibers. If these fibers were regular step index visible single-mode fibers, only 3 or 4 fibers can be aligned with the lens array at the same time. However, since the PCF we used has an MFD approximately 3 times greater than that of the regular step-index single-mode fiber, we were able to couple light into 12 fibers at the same time as shown in the far field pattern of the reflected fiber-coupled beams in Figure 19. The rms wavefront error of these beams is 0.046 wave as shown in Figure 20. This is also slightly better than the result of the regular step-index fiber array, where same amount of rms phase variation was observed for only 7 fibers. Taking into the second lens array this wavefront error is less than ~ 1/15 wave.

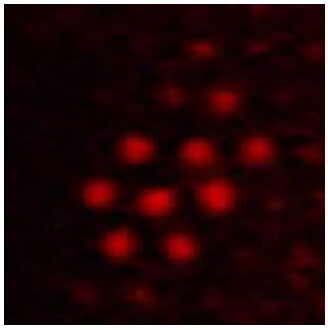

Figure 19: Far field pattern of coupled fiber beams for PCF array and MEMS Optical lens array.

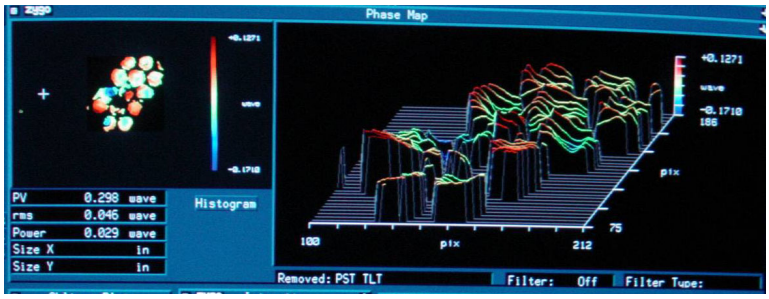

Figure 20: Phase map of PCF array. 12 beams coupled with PV = 0.298 wave, rms = 0.046 wave

5. FUTURE PLAN

5.1 Large MFD step-index single mode fiber array

We have demonstrated the advantage of a large MFD fiber array using the off-the-shelf PCF. However, it may be advantageous to use a custom large MFD conventional step-index single-mode fiber in the future 1000-channel fiber array development for the following reasons: (1) there is no precision cleaving and air-hole sealing process required if we use conventional fibers, (2) it has a flatter coupling efficiency response than PCF. The reason for (2) is because coupling efficiency changes as the overlap between the fiber mode pattern and the focused beam pattern changes; PCF has an MFD that is relatively independent of the wavelength, while the focused beam spot diameter is linearly proportional to the wavelength. This leads to a strong wavelength-dependent overlap between focused beam and fiber mode. In contrast, the MFD of a conventional step-index single-mode fiber is nonlinearly proportional to the wavelength and the overlap between fiber mode and focused beam is relatively independent of wavelength over an octave.

According to our survey, in principle, the large MFD step-index single mode fiber can be manufactured using existing fiber perform technology. The larger cladding diameter does increase the uncertainty of the concentricity of the fiber core and the cladding. To counter this effect, one can increase the fiber core diameter. A consequence of increasing core diameter is the increase of bending loss. This most likely will not be a problem since the fiber is short and straight in the array.

5.2 Mapping fiber positions and matched lens array

If the use of large MFD fiber still can not meet the alignment requirement another method is to map the fiber positions and layout the lens positions according to this fiber-position map. This is possible because the lens array fabrication technology normally can achieve a sub-micron position tolerance. If there is a gap between two fibers, then the same gap can be created between the corresponding lenslets. As a result, the filling factor of this lens array will be smaller than that of a uniform lens array. However, a typical gap is normally on the order of a few microns at most, while the cladding diameter is normally several hundred microns. So the percentage change in filling factor is relatively small.

6. SUMMARY AND CONCLUSIONS

We have demonstrated the feasibility of fabricating a single-mode fiber based spatial filter. Conventional single-mode fibers and large-MFD PCFs were used. We demonstrated an equilateral prism-confined fiber array structure and developed a Zygo-interferometer based lens array to fiber array alignment methodology. The experimental results show that the use of large-MFD fibers can significantly relax the fiber array fabrication tolerance. The best wavefront error of the spatial filter array measured in this report is approximately < 1/15 wave rms at 632.8 nm over 12 fibers. A PCF array is fairly more expensive to fabricate due to the extra process to cleave and seal two ends of all fibers with very tight length tolerance. Furthermore, the coupling-efficiency vs. wavelength curve of a PCF is not as flat as that of a conventional step-index single-mode fiber. The future plan is to use custom large-cladding, large MFD, step-index single-mode fibers to build the 1000 channel fiber array. A further option is to map out the fiber positions and custom make a lens array with matched positions.

ACKNOWLEDGEMENT

The research described in this paper was carried out at the Jet Propulsion Laboratory, California Institute of Technology, under a contract with the National Aeronautics and Space Administration. The authors would like to thank Francisco Aguayo for his technical assistance, Stuart Shaklan, Eugene Serabyn, Stefan Martin, and James K. Wallace for useful discussions and feedback.

REFERENCES

1. Bertrand Mennesson, Mike Shao, Bruce M. Levine, James K. Wallace, Duncan T. Liu, Eugene Serabyn, C. Unwin and Charles A. Beichman, "Optical Planet Discoverer: How to turn a 1.5 m Telescope into a Powerful Exo-planetary Systems Imager," Proc. SPIE Vol. 4860, P. 32-44, 2002.